Journal of Engineering Physics and Thermophysics, Vol. 75, No. 6, 2002

HEAT EXCHANGE IN A LAMINAR BUBBLE FLOW ON THE INITIAL PORTION OF A PLANE CHANNEL

A. P. Vasil'ev

UDC 536.24

Heat exchange on the initial portion of a plane channel with a laminar bubble flow under unstabilized-flow conditions is calculated by the methods of boundary-layer theory. Results of these calculations are compared. An analytical solution of the energy equation for stabilized flow is presented.

In channels of certain power installations for direct conversion of energy [1], there exists heat exchange in bubble flows of a liquid metal; however, because of the lack of interest in such flows, methods for calculating the heat exchange have not been developed.

We take the following model of a bubble flow: a viscous incompressible fluid is a carrier phase, and an ideal incompressible gas is a dispersed phase; between these phases, thermal equilibrium is retained.

The integral relationships of momenta and energy for the entire mixture have the form

$$\frac{d\delta^{**}}{dx} + (2\delta^{**} + \delta^{*})\frac{U_1'}{U_1} + \frac{\delta^{*}}{\rho_*} SS' = \frac{\tau_w}{\rho_1^0 U_1^2}, \tag{1}$$

$$\frac{d\delta_{t.lr}^{**}}{dx} + \delta_{t.lr}^{**}\frac{U_1'}{U_1(x)} + \alpha_1 \frac{\mu_1}{\rho_1^0 c_1 U_1(x)\,\Theta(x)} \int_0^{\delta_{t.lr}} \left(\frac{du_1}{dy}\right)^2 dy = \frac{q_w}{\rho_1^0 c_1 U_1(x)\,\Theta(x)}. \tag{2}$$

The thicknesses δ^{*}, δ^{**}, and $\delta_{t.lr}^{**}$ are determined by the equalities

$$\delta^{*} = \delta_1^{*} + S^2 \frac{\delta_2^{*}}{\rho_*}, \quad \delta^{**} = \delta_1^{**} + S^2 \frac{\delta_2^{**}}{\rho_*}, \quad \delta_1^{*} = \int_0^{\delta(x)} \alpha_1 \left(1 - \frac{u_1}{U_1}\right) dy,$$

$$\delta_2^{*} = \int_0^{\delta(x)} \alpha_2 \left(1 - \frac{u_2}{U_2}\right) dy, \quad \delta_1^{**} = \int_0^{\delta(x)} \alpha_1 \frac{u_1}{U_1}\left(1 - \frac{u_1}{U_1}\right) dy,$$

$$\delta_2^{**} = \int_0^{\delta(x)} \alpha_2 \frac{u_2}{U_2}\left(1 - \frac{u_2}{U_2}\right) dy, \quad \delta_{t.lr}^{**} = \int_0^{\delta_{t.lr}} \alpha_1 \frac{u_1}{U_1}\left(1 - \frac{\theta}{\Theta}\right)\left(1 + \frac{\alpha_2 \rho_2^0 c_2}{\alpha_1 \rho_1^0 c_1} S\right) dy.$$

Calculation of the friction and heat exchange on the initial portion implies the application, in addition to Eqs. (1) and (2), of the laws of conservation of mass and heat flux, provided that the profiles of velocities and temperature are known. These profiles can be selected by satisfying the following conditions on the wall and on the outer boundary of the dynamic and thermal boundary layers [2]:

Orenburg State University, Orenburg, Russia; email: OVASILIEV@YANDEX.RU. Translated from Inzhenerno-Fizicheskii Zhurnal, Vol. 75, No. 6, pp. 116–126, November–December, 2002. Original article submitted December 17, 2001; revision submitted April 26, 2002.

1062-0125/02/7506-1387$27.00

$$y = 0: \quad u_1 = u_2 = \theta = 0, \quad \frac{\partial^2 u_1}{\partial y^2} = \frac{\partial^2 u_2}{\partial y^2} = \frac{\partial^2 \theta}{\partial y^2} = 0;$$

$$y = \delta(x): \quad u_1 = U_1, \quad u_2 = U_2, \quad \frac{\partial u_1}{\partial y} = 0, \quad \frac{\partial u_2}{\partial y} = 0; \quad y = \delta_{t.lr}(x): \quad \theta = \Theta, \quad \frac{\partial \theta}{\partial y} = 0,$$

which results in the expressions

$$\frac{u_1}{U_1} = \frac{3}{2}\frac{y}{\delta} - \frac{1}{2}\left(\frac{y}{\delta}\right)^3, \quad \frac{u_2}{U_2} = \frac{3}{2}\frac{y}{\delta} - \frac{1}{2}\left(\frac{y}{\delta}\right)^3, \quad \frac{\theta}{\Theta} = \frac{3}{2}\frac{y}{\delta_{t.lr}} - \frac{1}{2}\left(\frac{y}{\delta_{t.lr}}\right)^3. \tag{3}$$

Let us assume that the content of the gas phase α_2 is independent of the transverse coordinate y, which is valid in the absence of transverse forces (of Zhukovskii or Magnus) acting on a bubble on the source side of the carrier phase. In this approximation, from the mass-flow-rate equation written for the running cross section of the channel, we find the law of change of the velocity in the potential part of the flow:

$$U_1(x) = U_1(0)\frac{1}{1 - A_1\dfrac{\delta(x)}{a}}, \quad A_1 = \frac{3}{8}. \tag{4}$$

Now we calculate the characteristics of the dynamic boundary layer, introduce the new variables $\eta = (\delta/a)^2$ and $\zeta = x/L$, and reduce Eq. (1) to the form

$$\frac{d\eta}{d\zeta} = 3\frac{1+\alpha_2}{\alpha_1}\frac{1}{A_2}\frac{L/a}{\mathrm{Re}}\frac{1 - A_1\sqrt{\eta}}{1 + \left(2 + \dfrac{A_1}{A_2}\right)\dfrac{A_1\sqrt{\eta}}{1 - A_1\sqrt{\eta}}}, \quad A_2 = \frac{39}{280}. \tag{5}$$

The initial conditions for Eq. (5) will be specified in the following form: $\zeta = 0$ and $\eta(\zeta) = 0$. The Reynolds number is here determined by the equality $\mathrm{Re} = aU_1(0)/\nu_1^0$.

Equation (5) describes the development of the dynamic boundary layer on the initial portion and it can be integrated irrespective of Eq. (2). Separating the variables in Eq. (5) and taking into account that the boundary layers converge ($\delta = a$) at the end of the dynamic initial portion $\zeta = 1$, we obtain

$$\frac{1}{3\dfrac{1+\alpha_2}{\alpha_1}\dfrac{1}{A_2}\dfrac{L_{dyn}/a}{\mathrm{Re}}}\int_0^1 \frac{d\eta}{\dfrac{1 - A_1\sqrt{\eta}}{1 + \left(2 + \dfrac{A_1}{A_2}\right)\dfrac{A_1\sqrt{\eta}}{1 - A_1\sqrt{\eta}}}} = \frac{1}{3\dfrac{1+\alpha_2}{\alpha_1}\dfrac{1}{A_2}\dfrac{L_{dyn}/a}{\mathrm{Re}}} J(1) = 1.$$

The length of the initial dynamic portion turns out to be equal to

$$\frac{L_{dyn}}{2a\,\mathrm{Re}} = \frac{J(1)}{6}\frac{1-\alpha_2}{1+\alpha_2}A_2. \tag{6}$$

Calculation of the integral gives

$$J(1) = \int_0^1 \frac{1 + \left(2 + \frac{A_1}{A_2}\right)\frac{A_1\sqrt{\eta}}{1 - A_1\sqrt{\eta}}}{1 - A_1\sqrt{\eta}}\, d\eta = 3.686 .$$

Setting $\alpha_2 = 0$ in Eq. (6), we find the length of the dynamic initial portion in the single-phase flow $L_{dyn}/(2a\ \mathrm{Re}) = 0.086$. If in this expression we determine the Reynolds number from the equivalent diameter, then the relative length of the dynamic-stabilization portion will turn out to be equal to $L_{dyn}/(2a\ \mathrm{Re_d}) = 0.043$, which is about four times larger than the calculation results obtained in [3]. Unfortunately, in [3] nothing has been said of the method used for determining the length L_{dyn}; therefore, it is impossible to explain this discrepancy. The results of calculations according to the Targ method ($L_{in}/(2a\ \mathrm{Re}) = 0.09$) are given in [4]. As is evident, the selected velocity profile describes quite accurately the dynamics of development of a viscous boundary layer.

Of interest is also the problem on pressure loss on the portion of dynamic stabilization of the flow (the pressure loss will be taken to mean only the dissipative component). The calculations performed on the basis of Eq. (6) lead to the following expression for the pressure loss on the initial portion:

$$\frac{\Delta P_{fr}}{\frac{\rho_1^0 U_1^2(0)}{2}} = (1 - \alpha_2)\int_0^1 \frac{1 + \left(2 + \frac{A_1}{A_2}\right)\frac{A_1\sqrt{\eta}}{1 - A_1\sqrt{\eta}}}{(1 - A_1\sqrt{\eta})^2\sqrt{\eta}}\, d\eta .$$

In this expression, the value of the integral is equal to 7.705.

The relation $\eta = \eta(\zeta)$ makes it possible to calculate the development of the thermal boundary layer on the initial portion. It should be borne in mind that the thermal core of the flow is not involved in the heat exchange until the thermal boundary layers converge. We consider the case where the thermal boundary layer is buried in the dynamic layer, i.e., $\delta_{t.lr} < \delta$ and $L_{t.lr} > L_{dyn}$.

Let us calculate the following quantities characterizing the thermal boundary layer:

$$\delta_{t.lr}^{**} = \frac{3}{20}\alpha_1\delta(x)\, h^2\left(1 - \frac{h^2}{14}\right), \quad \int_0^{\delta_{t.lr}}\left(\frac{du_1}{dy}\right)^2 dy = \frac{9}{4}\frac{U_1^2(x)}{\delta(x)}\left(h - \frac{2}{3}h^2 + \frac{h^2}{5}\right),$$

where $h = \delta_{t.lr}/\delta < 1$, and transform Eq. (2) at $z = h^2$ to the form

$$\frac{dz}{d\zeta} = \frac{L}{a}\frac{1}{\sqrt{\eta}\left(1 - \frac{z}{7}\right)}\left(B(\eta, z) - D(\eta, z)\frac{d\eta}{d\zeta} - E(\eta, z)\right), \tag{7}$$

here

$$B(\eta, z) = 10\frac{1 - \frac{3}{2}\alpha_2}{\alpha_1}\frac{1}{\mathrm{Pe}}\frac{1 - A_1\sqrt{\eta}}{\sqrt{\eta z}}; \quad D(\eta, z) = \frac{1}{2}\frac{a}{L}\left(1 - \frac{z}{14}\right)z\left(\frac{A_1}{1 - A_1\sqrt{\eta}} + \frac{1}{\sqrt{\eta}}\right);$$

$$E(\eta, z) = 15\alpha_1(1 + \alpha_2)\frac{\mathrm{Ec}}{\mathrm{Re}}\frac{1}{1 - A_1\sqrt{\eta}}\sqrt{\frac{z}{\eta}}\left(1 - \frac{2}{3}z - \frac{z^5}{5}\right).$$

The Re, Pe, and Ec numbers are determined from the conditions at the channel inlet:

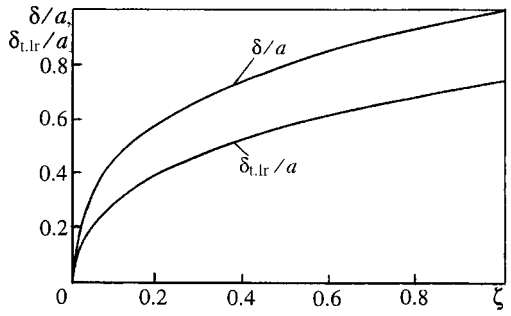

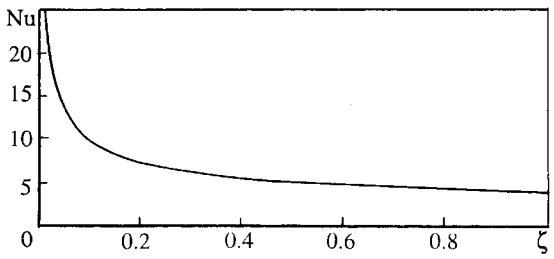

Fig. 1. Dependence of the thickness of the dynamic δ/a and thermal $\delta_{t.lr}$ boundary layers on the length $\zeta = x/L$ on the initial portion of the plane channel (the content of the gas phase in the flow is α = 20%).

Fig. 2. Dependence of the local Nusselt number Nu on ζ on the initial portion of dynamic stabilization of the flow, α = 20%.

$$\mathrm{Re} = \frac{\rho_1^0 U_1(0)\, a}{\mu_1^0}, \quad \mathrm{Pe} = \frac{U_1(0)\, a}{\dfrac{\lambda_{\mathrm{eff}}}{\rho_1^0 c_1}}, \quad \mathrm{Ec} = \frac{U_1^2(0)}{c_1 \Theta}.$$

Expressions (5) and (7) form a system of differential equations describing the development of the dynamic and thermal boundary layers on the initial channel portion to the point of convergence of the thermal boundary layer for the case where the thermal layer is buried in the dynamic layer.

The initial conditions for the functions sought are as follows: $z(\zeta)$, $\eta(\zeta)$:$\zeta = 0$, $z(0) = 1$, and $\eta(0) = 0$.

The system of equations (5) and (7) was integrated numerically. The solutions of this system converted to the thicknesses of the dynamic and thermal boundary layers are presented in Fig. 1. The initial data for calculation were as follows: channel height $2a$ = 0.02 m, velocity of the carrier phase (water) at the channel inlet $U_1(0)$ = 0.05 m/sec, volume gas content α_2 = 20%, Re = 1695, Pe = 4346, Ec = $6 \cdot 10^{-9}$ at Θ = 100°C, λ_1 = 0.683 W/(m·K), c_1 = 4220 J/(kg·K), $\nu_1^0 = 0.296 \cdot 10^{-6}$ m^2/sec, L_{dyn} = 1.934 m, and S = 1. The behavior of the curves in Fig. 1 shows that the thickness of the thermal boundary layer is smaller than that of the viscous boundary layer.

It is of greatest interest to elucidate the behavior of the heat-transfer coefficient on the portion of dynamic stabilization of the flow. Indeed, the heat-flux density on the tube wall can be calculated according to the Fourier heat-conduction law with the use of the coefficient of effective thermal conductivity of the bubble structure:

$$\frac{\lambda_1^0}{\lambda_{\mathrm{eff}}} = 1 + \frac{3}{2} \frac{\left(1 - \dfrac{\lambda_2^0}{\lambda_1^0}\right)\alpha_2}{1 - \left(1 - \dfrac{\lambda_2^0}{\lambda_1^0}\right)\sqrt[3]{\dfrac{9\pi}{16}\alpha_2^2}}.$$

For the heat-flux density on the channel wall we find

$$q_{\mathrm{w}} = -\lambda_{\mathrm{eff}} \left.\frac{\partial \theta}{\partial y}\right|_{y=0} = -\frac{3}{2}\Theta \frac{\lambda_{\mathrm{eff}}}{\delta_{\mathrm{t.lr}}(x)}.$$

On the other hand, the density can be determined according to the Newton–Richmann law $q_{\mathrm{w}} = -\beta(x)\Theta$ (Θ remains constant until the thermal boundary layers converge). Equating these expressions, for the local thermal-conductivity coefficient and the Nusselt number (Fig. 2) we find

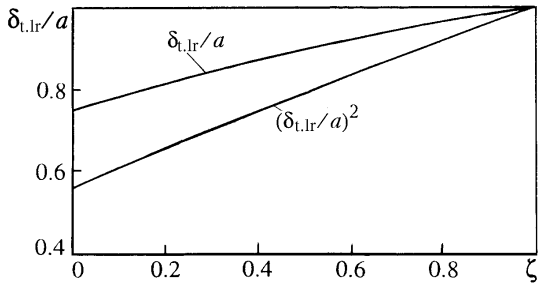

Fig. 3. Dependence of the reduced thickness of the thermal boundary layer $\delta_{t.lr}/a$ and the function $z = (\delta_{t.lr}/\delta)^2$ on ζ on the portion of thermal stabilization of the flow, $\alpha = 20\%$.

$$\beta(x) = \frac{3}{2}\frac{\lambda_{eff}}{\delta_{t.lr}(x)}, \quad \mathrm{Nu}(x) = \frac{\beta(x)\,2a}{\lambda_{eff}} = \frac{3}{\delta_{t.lr}(x)/a}.$$

One drawback of the velocity profile (3) is that after the completion of the dynamic stabilization flow it does not become the Poiseuille–Hagen profile. Thus, the mean flow velocity on the Poiseuille–Hagen profile is equal to $v = (2/3)U_{max}$, while Eq. (3) gives a value of $v = (7/12)U_{max}$, i.e., somewhat lower. We calculate the development of the thermal boundary layers on the portion $x \in [L_{dyn}; L_{t.lr}]$. The flow on this portion is stabilized, the dynamic boundary layers are converged, and $\delta = a$ ($\eta = 1$); therefore, the hydrodynamic processes no longer affect the thermal ones and Eq. (7) becomes independent. Setting $\eta = 1$, we rewrite Eq. (7) in the form

$$\frac{dz}{d\zeta} = \frac{L}{a}\frac{1}{\left(1-\frac{z}{7}\right)}(B(1,z) - E(1,z)). \tag{8}$$

The initial conditions for the function sought are $z(0) = z_0$, where z_0 is the solution of Eq. (7) at the point of convergence of the dynamic boundary layers, i.e., at $\zeta = 1$ (this parameter depends on both the gas content and the Pe number). In Eq. (8), the origin of the independent variable ζ is counted off from $x = L_{dyn}$.

By virtue of the smallness of the Eckert number, the heat release due to viscous dissipation in Eq. (8) can be neglected; then, upon integration, we find

$$\frac{2}{3}\left(\tau^{3/2} - \frac{3}{35}\tau^{5/2}\right)\Bigg|_{z_0}^{z} = 10\,\frac{L}{a}\,\frac{\left(1-\frac{3}{2}\alpha_2\right)(1-A_1)}{1-\alpha_2}\,\frac{\zeta}{\mathrm{Pe}}.$$

Since the portion of thermal stabilization of the flow ends at $z = 1$, with account for the previous equality for its length we obtain

$$\frac{L_{t.lr}}{2a\,\mathrm{Pe}} = \frac{16}{3}\,\frac{1-\alpha_2}{1-\frac{3}{2}\alpha_2}\,\left(\tau^{3/2} - \frac{3}{35}\tau^{5/2}\right)\Bigg|_{z_0}^{z} = \frac{16}{3}\,\frac{1-\alpha_2}{1-\frac{3}{2}\alpha_2}\,I(1,z_0), \quad I(1,z_0) = \left(\tau^{3/2} - \frac{3}{35}\tau^{5/2}\right)\Bigg|_{z_0}^{z=1}.$$

Thus, for the single-phase flow $z = z_0 = 0.957$, we have the function $I(1, z_0) = 0.036$, and the calculation of the length of the thermal initial portion gives the value $L_{t.lr}/(2a\ \mathrm{Pe}) = 0.00293$, $\mathrm{Pe} = 2960$. In [3], the value of $L_{t.lr}/(d_{eq}\,\mathrm{Pe}) = 0.0138$ is given for the length of the thermal initial portion, i.e., a fourfold discrepancy is observed. For the two-phase flow with the above-indicated initial data the calculations give the following values: $z_0 = 0.567$, $L_{t.lr}/(2a\ \mathrm{Pe}) = 0.031$, $\mathrm{Pe} = 4346$; the absolute length of the thermal initial portion increases with increase in the gas content. It should be noted that this length is sensitive to the thermal conductivity of the dispersed phase.

Noteworthy is the fact that after the completion of the dynamic stabilization of the flow the character of growth of the thickness of the thermal boundary layer changes and becomes almost linear (Fig. 3, the length of the

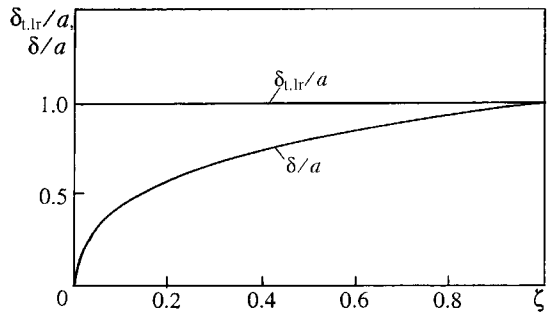

Fig. 4. Dependence of the thickness of the thermal $\delta_{t.lr}/a$ and dynamic δ/a boundary layers on ζ on the initial portion (the dynamic layer is buried in the thermal layer), α = 20%.

thermal initial portion was taken to be equal to $L_{t.lr}(2a\mathrm{Pe}) = 0.031$). The total length of the portion of thermal stabilization of the flow (from the channel inlet) is determined by the equality

$$\frac{L_\Sigma}{2a} = \frac{L_{dyn}}{2a} + \frac{L_{\grave{o}}}{2a} = \frac{J(1)}{6} A_2 \frac{1-\alpha_2}{1+\alpha_2} \mathrm{Re} + \frac{16}{3} \frac{1-\alpha_2}{1-\frac{3}{2}\alpha_2} I(1, z_0)\, \mathrm{Pe}\,.$$

The function $z = (\delta_{t.lr}/a)^2$ makes it possible to calculate the dependence of the local Nusselt number Nu(ζ) on the considered portion. The calculations show a continuous decrease in the heat-transfer coefficient and in the Nusselt number to a value of Nu = 3 at the point of convergence of the thermal layers; this fact is explained by the growth in the thickness of the thermal boundary layer along the flow.

Let us calculate the thermal boundary layer for the case $\delta_{t.lr} > \delta$ where the dynamic boundary layer is buried in the thermal boundary layer and, consequently, $L_{dyn} > L_{t.lr}$. This situation occurs, for example, in two-phase liquid-metal flows.

The equation of the dynamic boundary layer (5) holds true under these conditions, too, while Eq. (2), upon calculating all the characteristics of the thermal boundary layer with account for the inequality $\delta(x) < \delta_{t.lr}(x)$ and for the neglect of the volume heat release due to viscous dissipation, is reduced to the form ($h = \delta_{t.lr}/\delta$)

$$\frac{dh}{d\zeta} = \frac{L}{a} \frac{1}{a_1 \Psi(h)} \frac{1}{\sqrt{\eta}} \left\{ (1 - a_1 A_1 \sqrt{\eta}) \frac{3}{2} \left(1 - \frac{3}{2}\alpha_2\right) \frac{1}{\mathrm{Pe}\, h \sqrt{\eta}} - \alpha_1 \Phi(h) \left(1 + \frac{\sqrt{\eta}}{1 - A_1\sqrt{\eta}}\right) \frac{a}{L} \frac{1}{2} \frac{1}{\sqrt{\eta}} \frac{d\eta}{d\zeta} \right\}, \qquad (9)$$

where

$$\Phi(h) = -\frac{3}{8} + \frac{3}{8} h + \frac{3}{20} \frac{1}{h} + \frac{29}{1120} \frac{1}{h^3}; \quad \Psi(h) = \frac{3}{8} - \frac{3}{20} \frac{1}{h^2} - \frac{87}{1120} \frac{1}{h^4}.$$

The system of equations (5) and (9) for the dynamic and thermal boundary layers under the considered conditions can be integrated numerically. The initial conditions for the functions $\eta(\zeta)$ and $h(\zeta)$ are specified in the form $\zeta = 0$, $\eta(\zeta) = 0$, and $h(\zeta) = 1$.

Figure 4 illustrates the solutions of (5) and (9) converted to the relative thicknesses of the dynamic and thermal boundary layers. As the carrier phase we selected liquid-metal gallium with α_2 = 20% for a = 0.01 m and $L = L_{dyn}$ = 3.272 m. The thermophysical characteristics of liquid gallium were prescribed at $\Theta = 300^{o}$C and were equal to $\nu = 1.743 \cdot 10^{-7}$ m^2/sec, ρ = 5095 kg/m^3, λ = 13 W/(m·^{o}C), and c = 1300 J/(kg·^{o}C). The criteria of the problem were Re = 2869 and Pe = 295.

From Fig. 4 it follows that on the initial channel portion the thermal boundary layer ($\delta_{t.lr}/a$), grows very rapidly, while the dynamic boundary layer grows smoothly (δ/a), so that thermal stabilization is completed almost near the inlet cross section of the channel $L_{t.lr} = 0$.

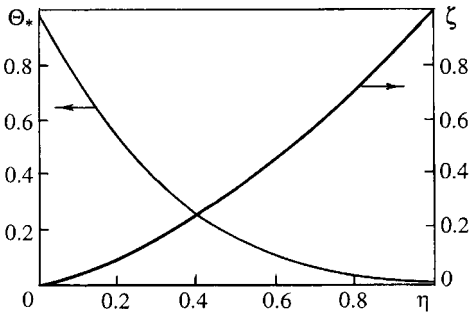

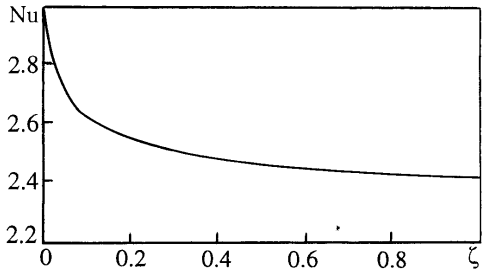

Fig. 5. Dependence of the reduced temperature $\Theta_* = \Theta(\eta)/\Theta(0)$ and the reduced longitudinal coordinate $\zeta = \zeta(\eta)$ on the square of the reduced thickness of the dynamic boundary layer $\eta = (\delta/a)^2$.

Fig. 6. Dependence of the local Nusselt number Nu on ζ (the flow is dynamically stabilized).

After the convergence of the thermal boundary layers, the temperature on the flow axis begins to change. After the calculation of the convective flows and integration of the resulting equation, from the heat-balance equation $dQ(x)/dx = q_w$ we find the law of change of the temperature on the flow axis:

$$\left|\frac{\Theta(\eta(\zeta))}{\Theta(0)}\right| = \frac{\chi(0)}{\chi(\sqrt{\eta})}(1 - A_1\sqrt{\eta})\exp\left[-\frac{5}{6}\frac{1}{1+\alpha_2}A_2\frac{\mathrm{Re}}{\mathrm{Pe}}K(0,\eta)\right],$$

where

$$K(0,\eta) = \int_0^{\eta}\frac{1+\left(2+\dfrac{A_1}{A_2}\right)\dfrac{A_1\sqrt{x}}{1-A_1\sqrt{x}}}{\Phi(\sqrt{x})(1-A_1\sqrt{x})^2}dx;\quad \chi(\sqrt{\eta}) = 1 + \frac{1}{4}\eta + \frac{1}{5}\eta^2.$$

Figure 5 shows the dependence of the reduced temperature $\Theta_* = \Theta(y)/\Theta(0)$ on the variable $\eta = (\delta/a)^2$ and, for the convenience of passage to the longitudinal coordinate ζ, the plot of the function $\zeta = \zeta(\eta)$. In the calculations it was assumed that $\eta_0 = 0$. The other data corresponded to those given above.

After the convergence of the thermal boundary layers, the Newton–Richmann law is characterized by the mass-mean temperature (mixing temperature)

$$\bar{\theta} = \frac{2}{\dot{m}_1 c_1 + \dot{m}_2 c_2}\int_0^a(\rho_1 u_1 c_1 + \rho_2 u_2 c_2)\,\theta(y)\,dy = \Theta(x)\frac{1 - \dfrac{6}{25}\left(\dfrac{\delta}{a}\right)^2 + \dfrac{9}{525}\left(\dfrac{\delta}{a}\right)^4}{1 - A_1\dfrac{\delta}{a}},$$

where $\dot{m}_1$ and $\dot{m}_2$ are the mass flow rates of the phases. In calculating, it was taken into account that $\rho_* > 1$.

The local heat-transfer coefficient and the Nusselt number determined from the mass-mean temperature are as follows:

$$\beta(x) = \frac{3}{2}\frac{\lambda_{\mathrm{eff}}}{a}\frac{1 - A_1\dfrac{\delta}{a}}{1 - \dfrac{6}{25}\left(\dfrac{\delta}{a}\right)^2 + \dfrac{9}{525}\left(\dfrac{\delta}{a}\right)^4},\quad \mathrm{Nu}(x) = \frac{\beta 2a}{\lambda_{\mathrm{eff}}} = 3\frac{1 - A_1\dfrac{\delta}{a}}{1 - \dfrac{6}{25}\left(\dfrac{\delta}{a}\right)^2 + \dfrac{9}{525}\left(\dfrac{\delta}{a}\right)^4}.$$

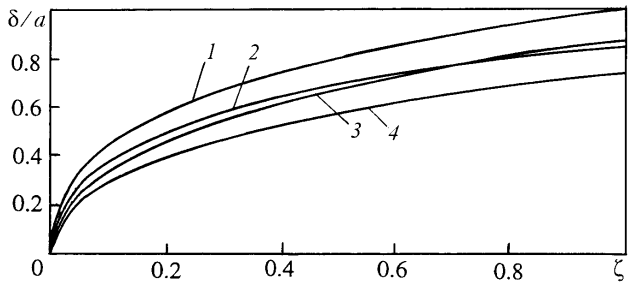

Fig. 7. Reduced thickness of the dynamic (curves 1 and 2) and the thermal (curves 3 and 4) boundary layers as a function of ζ on the portion of dynamic stabilization of the flow: 2 and 3 are the single-phase layers; 1 and 4 are the two-phase layers.

In particular, after the convergence of the dynamic boundary layers ($\delta = a$) the Nusselt number ceases to change along the channel length and it is equal to Nu = 2.413 (Fig. 6).

Now we investigate the conditions that ensure a particular scheme of development of the thermal boundary layer. We consider the case where $\delta_{t.lr} < \delta$. Let the function $z(\zeta)$ from Eq. (7) be decreasing over the entire interval $\zeta \in [0; 1]$. To do this requires the derivative $dz/d\zeta < 0$. Applying this condition to the right-hand side of Eq. (7) at the point $\zeta = 0$ and taking into account that $z(0) = 1$, we obtain the following condition:

$$\mathrm{Pr} = \frac{\mathrm{Pe}}{\mathrm{Re}} > \mathrm{Pr}_{cr} = \frac{5}{2}\frac{1 - \frac{3}{2}\alpha}{1 + \alpha}.$$

Thus, for $\mathrm{Pr} > 5/2$ (in the case of the single-phase flow) the scheme of development of the boundary layers in which $\delta_{t.lr} < \delta$ will be implemented, whereas for $\mathrm{Pr} < \mathrm{Pr}_{cr}$, the scheme with $\delta_{t.lr} > \delta$ will be implemented (for the velocity and temperature profiles taken in the boundary layers).

Now we consider the problem on the influence of the two-phase structure of the flow on the development of the boundary layers on the initial portion of the channel.

Figure 7 presents results of the calculation of the thicknesses of the dynamic and thermal boundary layers for the single- and two-phase flows with $\alpha = 20\%$. The calculations were performed with $L = L_{dyn}$; the convergence of the dynamic two-phase boundary layer was observed at $\zeta = 1$; the boundary layers in the single-phase flow continued to thicken, i.e., the length of the dynamic initial portion of the single-phase flow was larger than the length of the two-phase flow.

It is evident from the plots that the thickness of the dynamic two-phase boundary layer (curve 1) is larger than the thickness of the dynamic single-phase boundary layer (curve 2) and grows more rapidly than that of the latter. This rate of growth of the thickness can be explained by the higher effective viscosity of the two-phase flow compared to the single-phase flow. Indeed, from the formula $\mu_{eff} = \mu_1^0(1 + \alpha_2)$ it follows that with increase in the volume gas content of the dispersed phase, the effective flow viscosity increases, thus causing the above phenomenon. However, the thickness of the thermal single-phase boundary layer (curve 3) exceeds that of the two-phase layer (curve 4) and has a high rate of growth, which can be explained by the higher value of the thermal-conductivity coefficient of the single-phase flow compared to that of the two-phase flow, in view of which the Péclet number, controlling the rate of growth in the thermal boundary layer, turns out to be smaller in the single-phase flow. Because of this, the right-hand side of the equation for the thermal boundary layer becomes larger in the case of the single-phase flow, thus determining the increase in the growth rate of the thickness of the thermal boundary layer precisely in this flow. In a qualitative sense, this pattern is explained by the fact that the temperature field in the single-phase flow diffuses more rapidly than in the two-phase flow, wherein the presence of gas inclusions with a low thermal conductivity retards the process of diffusion of heat. The distribution pattern is reversed if the thermal conductivity of the material of inclusions exceeds that of the carrier phase: in this case the thickness of the thermal boundary layer in the two-phase flow turns out to be larger than in the single-phase flow.

It should also be noted that the heat-transfer coefficient β is higher in the single-phase flow than in the two-phase flow: the dispersed phase leads to a decrease of about 30% in it under the conditions of the example described.

Now we consider the calculation of β for dynamically stabilized flow. When $x < 0$, the channel walls of height $2a$ are adiabatically insulated, whereas when $x \geq 0$, their temperature changes abruptly and becomes equal to $T_w > T_{liq}$.

The stationary problem of convective heat exchange is described by the energy equation which can be written for each of the phases as:

$$\rho_1 c_1 (\mathbf{v}_1 \cdot \nabla)\, \theta = \lambda_1 \nabla^2 \theta\,, \quad \rho_2 c_2 (\mathbf{v}_2 \cdot \nabla)\, \theta = \lambda_2 \nabla^2 \theta\,. \tag{10}$$

Let us assume that the longitudinal velocities for each of the phases in stabilized flow are described by the following profiles:

$$u_1(y) = U_1 \left(1 - \left(\frac{y}{a}\right)^2\right), \quad u_2(y) = U_2 \left(1 - \left(\frac{y}{a}\right)^2\right).$$

If we neglect the heat flux along the channel due to molecular heat conduction compared to the heat flux due to convection (which is true at large Péclet numbers), we can discard the second derivative with respect to the variable x on the right-hand side of the energy equation. Then, combining Eqs. (10) and introducing the notation $\lambda_{eff} = \lambda_1 + \lambda_2$, for $\mathrm{Pe} = U_1 a / a_{eff}$ and

$$a_{eff} = \frac{\lambda_{eff}}{\alpha_1 \rho_1^0 c_1 \left(1 + \dfrac{\rho_2^0}{\rho_1^0} \dfrac{\alpha_2}{\alpha_1} \dfrac{c_2}{c_1} S\right)}$$

we have

$$\left(1 - \left(\frac{y}{a}\right)^2\right) \frac{\partial \theta}{\partial x} = \frac{a}{\mathrm{Pe}} \frac{\partial^2 \theta}{\partial y^2}\,. \tag{11}$$

Equation (11) will be solved by the method of separation of variables; to do this, we represent the function sought in the form $\theta = (x, y) = \varphi(x)\psi(y)$ and, having substituted it into Eq. (11), after separation of the variables we obtain

$$\frac{\mathrm{Pe}}{a} \frac{\varphi'(x)}{\varphi(x)} = \frac{\psi''(y)}{\left(1 - \left(\dfrac{y}{a}\right)^2\right) \psi(y)} = -l^2\,.$$

Equation (11) is reduced to the system of two ordinary differential equations

$$\varphi'(x) + \frac{a}{\mathrm{Pe}} \varphi'(x)\, l^2 = 0\,, \quad \psi''(x) + \left(1 - \left(\frac{y}{a}\right)^2\right) \psi(y) = 0\,. \tag{12}$$

The solution of the first equation of (12) is the function

$$\varphi(x) = C \exp\left(-\frac{a l^2}{\mathrm{Pe}} x\right),$$

where C is the integration constant to be determined.

We will seek the solution of the second equation of (12) in the form of the sum of a power series which is symmetric about y:

$$\psi(y) = A_0 + A_2\left(\frac{y}{a}\right)^2 + A_4\left(\frac{y}{a}\right)^4 + \ldots + A_{2k}\left(\frac{y}{a}\right)^{2k} = \sum_{p=0}^{k} A_{2p}\left(\frac{y}{a}\right)^{2p},$$

$$\psi''(y) = \frac{1}{a^2}\sum_{p=0}^{k} 2p\,(2p-1)\,A_{2p}\left(\frac{y}{a}\right)^{2p-2}.$$

We substitute these series into Eq. (12) and introduce the notation $\gamma = a^2 l^2$; then, comparing the coefficients y/a of the same power, we obtain the following system of recurrence equations for determining the unknown coefficients:

$$1\cdot 2A_2 + \gamma A_0 = 0,$$

$$3\cdot 4A_4 + \gamma A_2 - \gamma A_0 = 0,$$

$$5\cdot 6A_6 + \gamma A_4 - \gamma A_2 = 0,$$

.....

$$(2k-1)\cdot 2kA_{2k} + \gamma A_{2k-2} - \gamma A_{2k-4} = 0.$$

The coefficient A_0 is set equal to 1; then from this system we can successively find all the other coefficients of the series:

$$A_2 = -\frac{\gamma}{1\cdot 2}, \quad A_4 = \frac{\gamma}{3\cdot 4}\left(1 + \frac{\gamma}{1\cdot 2}\right), \ldots$$

i.e.,

$$A_{2p} = \frac{\gamma}{(2k-1)\cdot 2k}\,(A_{2k-4} - A_{2k-2}). \tag{13}$$

Consequently, the particular solution of Eq. (12) has the form

$$\theta(x, y) = C\exp\left(-\frac{\gamma}{\mathrm{Pe}}\frac{x}{a}\right)\sum_{p=0}^{k} A_{2p}\left(\frac{y}{a}\right)^{2p}. \tag{14}$$

The general solution of Eq. (11) will be sought in the form of an infinite sum of the particular solutions (14):

$$\theta(x, y) = \sum_{n=0}^{\infty}\theta_n(x, y) = \sum_{n=0}^{\infty} C_n\exp\left(-\frac{\gamma_n}{\mathrm{Pe}}\frac{x}{a}\right)\sum_{p=0}^{k} A_{2p}\left(\frac{y}{a}\right)^{2p}. \tag{15}$$

The separation constant γ will be determined from the boundary conditions of the first kind on the channel walls (isothermal walls) $y = \pm a$ and $\theta(x, a) = 0$, which results in the equation

$$A_0 + A_2 + \ldots + A_{2k} = 0. \tag{16}$$

Substituting here the coefficients of the series expressed by the unknown γ, we obtain the algebraic equation of the kth degree relative to the unknown γ with real coefficients.

According to the main theorem of algebra, such an equation has exactly k roots and some of them will be complex-conjugate. Of all the roots of Eq. (16), we select only the real positive roots, since only these roots ensure the condition of convergence of the solution at positive infinity. Let there be m such roots, $m \le k$.

We find the coefficients C_n of series (15). To do this we turn to the conditions at the channel inlet: when $x = 0$, $\theta(0, y) = \Theta F(y/a)$. Here $F(y/a)$ is the prescribed function which is even relative to y and Θ is the excess temperature on the flow axis. We expand the function $F(y/a)$ in a Taylor series:

$$F\left(\frac{y}{a}\right) = F(0) + \frac{F''(0)}{2!}\left(\frac{y}{a}\right)^2 + \frac{F^{(4)}(0)}{4!}\left(\frac{y}{a}\right)^4 + \ldots, \quad F(0) = 1.$$

When $x = 0$, the solution (15) takes the form

$$\theta\left(0, \frac{y}{a}\right) = \sum_{n=0}^{\infty} C_n \sum_{p=0}^{k} A_{2p}\left(\frac{y}{a}\right)^{2p} = \Theta\left(1 + \frac{F'(0)}{1!}\frac{y}{a} + \frac{F''(0)}{2!}\left(\frac{y}{a}\right)^2 + \ldots\right),$$

or, changing the order of summation, we rewrite it as follows:

$$\sum_{p=0}^{k}\left(\frac{y}{a}\right)^{2p}\sum_{n=0}^{m} C_n A_{2p}(\gamma_n) = \Theta \sum_{p=0}^{k}\frac{F^{(2p)}(0)}{(2p)!}\left(\frac{y}{a}\right)^{2p}.$$

Whence we obtain the following linear system of equations for determining the unknown coefficients C_n:

$$C_0 \cdot 1 + C_1 \cdot 1 + \ldots + C_{m-1} \cdot 1 = \Theta,$$

$$C_0 \cdot A_2(\gamma_0) + C_1 \cdot A_2(\gamma_1) + \ldots + C_{m-1} \cdot A_2(\gamma_{m-1}) = \frac{F^{(2)}(0)}{2!}\Theta,$$

.....,

$$C_0 \cdot A_{2k}(\gamma_0) + C_1 \cdot A_{2k}(\gamma_1) + \ldots + C_{m-1} \cdot A_{2k}(\gamma_{m-1}) = \frac{F^{(2k)}(0)}{(2k)!}\Theta.$$

We separate linearly independent equations ($m \times m$ matrix) and will count off the subscript m from unity and not from zero; then the system of linear equations is conveniently written as follows:

$$C_1 + C_2 + \ldots + C_m = \Theta,$$

$$C_1 \cdot A_2(\gamma_1) + C_1 \cdot A_2(\gamma_2) + \ldots + C_m \cdot A_2(\gamma_m) = \frac{F^{(2)}(0)}{2!}\Theta,$$

.....,

$$C_1 \cdot A_{2m-2}(\gamma_1) + C_1 \cdot A_{2m-2}(\gamma_2) + \ldots + C_m \cdot A_{2m-2}(\gamma_m) = \frac{F^{(2m-2)}(0)}{(2m-2)!}\Theta.$$

Let $a_{i,j} = A_{2i-2}(\gamma_j)$ be the elements of the matrix $A = \|a_{i,j}\|$, $i \le m$ and $j \le m$, and B be the vector composed of the right-hand sides of the system of equations; then its solutions can be represented in matrix form: $C^* = A^{-1}B/\Theta$, where A^{-1} is the inverted matrix.

With account for the coefficients obtained, the solution of (11) takes the form

$$\theta_*(x, y) = \frac{\theta(x, y)}{\Theta} = \sum_{n=1}^{m} C_n^* \exp\left(-\frac{\gamma_n}{\mathrm{Pe}}\frac{x}{a}\right)\sum_{p=0}^{k} A_{2p}\left(\frac{y}{a}\right)^{2p}.$$

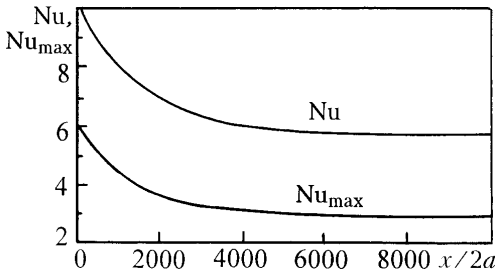

Fig. 8. Dependence of the Nusselt numbers Nu and Nu_{max} on $x/2a$ on the initial thermal portion (the flow is dynamically stabilized).

We calculated the density of the heat flux on the wall according to the Fourier heat-conduction law:

$$q_w = -\lambda_{eff}\left.\frac{\partial\theta}{\partial y}\right|_{y=a} = -4\lambda_{eff}\frac{\Theta}{2a}\sum_{n=1}^{m} C_n^* \exp\left(-\frac{\gamma_n}{Pe}\frac{x}{a}\right)\sum_{p=1}^{k} pA_{2p}(\gamma_n).$$

On the other hand, the same heat flux can be represented according to the Newton–Richmann law as $q_w = \beta\Delta t$. The value of the coefficient β will, obviously, depend on the way of selecting the characteristic temperature difference between the wall and the flow.

Thus, when $\Delta t = \Theta\theta_*(x, 0)$, i.e., in selecting the maximum temperature head between the wall and the flow axis, the heat-flux density turns out to be equal to

$$q_w = -\Theta\theta_*(x, 0) = -\Theta\sum_{n=1}^{m} C_n^* \exp\left(-\frac{\gamma_n}{Pe}\frac{x}{a}\right),$$

and for the Nusselt number we obtain the following expression:

$$Nu_{max} = \frac{\beta_{max}2a}{\lambda_{eff}} = 4\frac{\sum_{n=1}^{m} C_n^* \exp\left(-\frac{\gamma_n}{Pe}\frac{x}{a}\right)\sum_{p=1}^{k} pA_{2p}(\gamma_n)}{\sum_{n=1}^{m} C_n^* \exp\left(-\frac{\gamma_n}{Pe}\frac{x}{a}\right)}.$$

By selecting the mass-mean temperature

$$\bar{\theta} = \frac{\Theta}{a}\int_0^1 \theta_*(x, \varepsilon)(1-\varepsilon^2)\,d\varepsilon = \frac{2}{3}\frac{\Theta}{a}\sum_{n=1}^{m} C_n^* \exp\left(-\frac{\gamma_n}{Pe}\frac{x}{a}\right)\left(1 + 3\sum_{p=1}^{k}\frac{A_{2p}(\gamma_n)}{(2p+1)(2p+3)}\right),$$

as the determining one, from the equality $q_w = \beta\bar{\theta}$ we find the Nusselt number:

$$Nu = \frac{\beta 2a}{\lambda_{eff}} = 6\frac{\sum_{n=1}^{m} C_n^* \exp\left(-\frac{\gamma_n}{Pe}\frac{x}{a}\right)\sum_{p=1}^{k} pA_{2p}(\gamma_n)}{\sum_{n=1}^{m} C_n^* \exp\left(-\frac{\gamma_n}{Pe}\frac{x}{a}\right)\left(1 + 3\sum_{p=1}^{k}\frac{A_{2p}(\gamma_n)}{(2p+1)(2p+3)}\right)}.$$

The results of calculation of the Nusselt number over the channel length are presented in Fig. 8. The initial data for the calculation were identical to those given in Fig. 1. We had Re = 1689 and Pe = 4346. The initial distribution of

the excess temperature Θ in the flow was taken to be uniform. We solved Eq. (16) for $k = 8$ (when the degrees of the equation are higher the expenditure of computer time is unjustifiably large); here, two real roots, $\gamma_1 = 2.827$ and $\gamma_2 = 27.23$, were obtained. The coefficients C_n^* reduced to the maximum temperature head at the channel inlet were $C_1^* = 1.116$ and $C_2^* = -0.116$ under these conditions. The behavior of the Nusselt number on the channel length is qualitatively the same as in the case of calculation within the framework of the boundary-layer theory.

The largest Nusselt number in Fig. 8 corresponds to the mass-mean temperature, whereas the smallest Nusselt number corresponds to the maximum characteristic temperature between the channel wall and the flow axis: $\mathrm{Nu}(\infty) = 5.65$ and $\mathrm{Nu}_{\max}(\infty) = 2.858$. We should note that at infinity the Nusselt number is independent of the gas content.

It is of interest to compare the results obtained to those available in the literature. Thus, Nu = 5.95 calculated from the mean-flow-rate temperature for the single-phase flow in a plane channel with isothermal walls is given in [5]. The calculation of the Nusselt number in the single-phase flow according to the method presented leads to a value of Nu = 5.65. At the same time, the calculation performed according to the boundary-layer theory gives $\mathrm{Nu}_{\max} = 3$ (Fig. 3). The analytical solution results in $\mathrm{Nu}_{\max}(\infty) = 2.858$. As we see, the agreement is quite satisfactory in both cases.

The two-phase structure of the flow has an effect primarily on the Péclet numbers of the problem, which determine the length of the thermal initial portion of the channel (the presence of the dispersed phase leads to an increase in this length).

NOTATION

δ, δ^*, δ^{**}, and $\delta_{\mathrm{t.lr}}^{**}$, boundary-layer, displacement, momentum-loss, and energy-loss thicknesses; S, coefficient of slippage of the phases; ρ_i and ρ_i^0, reduced and true densities of the ith phase; ρ_*, dimensionless density; u_i and U_i, local velocity and velocity on the flow axis of the ith phase; v, mean velocity; θ and Θ, local and maximum excess temperatures; $\bar{\theta}$, mass-mean temperature; c_i, heat capacity of the ith phase; α, volume gas content; x and y, Cartesian longitudinal and transverse coordinates; a, half-height of the channel; d, diameter; L, channel length; A_1 and A_2, profile coefficients; $J(y)$, $I(1, z)$, and $K(0, y)$, profile integrals; ΔP, pressure loss; τ, viscous friction stress; ζ and ε, reduced longitudinal and transverse coordinates; $\eta(\zeta)$, $z(\zeta)$, and $h(\zeta)$, functions of the boundary layers; Re, Pr, Pe, Ec, and Nu, Reynolds, Prandtl, Péclet, Eckert, and Nusselt numbers; B, D, E, Φ, Ψ, and χ, functions of the system of boundary-layer equations; μ_{eff} and μ_1^0, effective and true dynamic viscosities of the carrier phase; ν, coefficient of kinematic viscosity; λ_i^0 and λ_{eff}, true thermal conductivity of the ith phase and effective thermal conductivity of the mixture; q, heat-flux density; Q, convective heat flux; β, heat-transfer coefficient; a_{eff}, effective thermal-diffusivity coefficient; l, separation constant; $\varphi(x)$ and $\psi(y)$, functions of the Fourier method; $F(y)$, function assigning the temperature distribution at the channel inlet; A, matrix of the coefficients in the system of equations; B, vector of the free terms of the equations of the system; C_k, A_k, and C_k^*, coefficients of the series; γ_k, roots of the characteristic equation; Δt, characteristic temperature; p, m, k, and n, natural numbers. Subscripts: i, phase subscript; $i = 1$, carrier phase; $i = 2$, dispersed phase; j, natural number; w, parameter on the channel wall; eff, effective parameter; *, reduced parameter; t.lr, thermal boundary layer; dyn, dynamic boundary layer; in, parameter of the initial portion; fr, friction; liq, liquid; d, diameter; eq, equivalent; cr, critical; 0, initial value of the function; Σ, total value; max, maximum. Superscripts: 0, true parameter; $'$ and $''$, derivatives; * and **, parameters of the boundary layer.

REFERENCES

1. A. P. Vasil'ev, V. A. Bondarenko, D. A. Tarakov, et al., *Kholod. Tekh.*, No. 12, 22–24 (1991).
2. I. L. Povkh, *Engineering Hydromechanics* [in Russian], Leningrad (1976).
3. V. K. Koshkin (ed.), *Heat Transfer in Power Installations of Spacecraft Vehicles* [in Russian], Moscow (1975).
4. B. T. Emtsev, *Engineering Hydromechanics* [in Russian], Moscow (1987).
5. W. M. Kays, *Convective Heat and Mass Transfer* [Russian translation], Moscow (1972).